

Article

Novel Understandings of Biomineralization in Backfill Materials: A Fundamental Investigation of Coal Gangue and Fly Ash Impact on *B. pasteurii* to Enhance Material Properties

Shijie Guo ^{1,2}, Alessandro Pasquale Fantilli ² , Hao Yan ^{1,*}, Kai Sun ¹ and Luwei Ding ¹¹ School of Mines, China University of Mining & Technology, Xuzhou 221116, China; sxjxgsj@gmail.com (S.G.)² Department of Structural, Building and Geotechnical Engineering, Politecnico di Torino, Corso Duca degli Abruzzi 24, 10129 Torino, Italy

* Correspondence: haoyan@cumt.edu.cn

Abstract: This paper proposes a fundamental investigation of coal gangue and fly ash impact on *B. pasteurii* to enhance the properties of backfill materials. The goal is to obtain effective microbial mineralization and potential mechanical properties of coal gangue and fly ash as backfill materials and to mitigate the impact of the most common binders used in the backfill material of mines. Micro-scale mineralization was performed with *B. pasteurii* bacteria using microbially induced carbonate precipitation (MICP) technology to clarify solid waste impact on *B. pasteurii* and to bind coal gangue and fly ash. Several tests were carried out to analyze the behavior of *B. pasteurii*, especially when it coexists with these two waste materials separately. In such cases, it was possible to observe a reduction in mineralization initiation time with respect to the natural mineralization of the MICP technology. Moreover, at the macro-scale, the new mineralized backfilling material shows good workability in the fresh state, whereas the strength at 28 days is 5.34 times higher than that obtained with non-mineralized coal gangue and fly ash.

Keywords: solid waste; backfill mining; microbially induced carbonate precipitation; mineralization initiation time; micro-scale mineralization



Citation: Guo, S.; Fantilli, A.P.; Yan, H.; Sun, K.; Ding, L. Novel Understandings of Biomineralization in Backfill Materials: A Fundamental Investigation of Coal Gangue and Fly Ash Impact on *B. pasteurii* to Enhance Material Properties. *Appl. Sci.* **2024**, *14*, 799. <https://doi.org/10.3390/app14020799>

Academic Editor:
Nikolaos Koukoulzas

Received: 17 November 2023

Revised: 13 January 2024

Accepted: 15 January 2024

Published: 17 January 2024



Copyright: © 2024 by the authors. Licensee MDPI, Basel, Switzerland. This article is an open access article distributed under the terms and conditions of the Creative Commons Attribution (CC BY) license (<https://creativecommons.org/licenses/by/4.0/>).

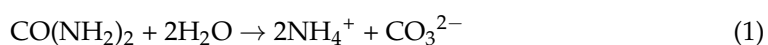
1. Introduction

Coal gangue (CG) is a solid waste byproduct of the coal mining process. The mass of CG, which is approximately 15–20% that of coal produced yearly, is one of the largest amounts of solid waste in China. Currently, 1500 gangue mountains have been formed in China, storing more than 3 billion tons of unused CG, covering an area of nearly 20,000 hectares [1]. Similarly, fly ash (FA) constitutes the majority of coal combustion products (CCPs), accounting for approximately 40–90% of the total CCPs. For every 4 tons of coal burned, 1 ton of CCPs is generated, and the worldwide production of CCPs in 2019 was approximately 1.2 billion tons per year [2,3]. The disposal of CG and FA not only occupies a considerable amount of land, but, due to long-term weathering and leaching, it also causes the accumulation of heavy metals and water pollution in the surrounding soil [4]. Moreover, FA can also produce dust pollution [5], which potentially contaminates the atmosphere.

Accordingly, part of the green mining technology consists of the cementation of solid waste resources, such as CG and FA, and using them to backfill the goaf of coal mines. The solid waste is prepared as a slurry composite and pumped into the underground goaf of the coal mine through backfilling pipelines [6]. The confined environment of the goaf could limit, to some extent, the dispersion of any mobile contaminants leaching from the backfilling material [7,8]. This technology can reduce hazards caused by CG and FA, as well as largely solve a series of other ecological problems, such as the destruction of the underground water system and subsidence due to the traditional method of mining.

Specific binders, such as cement and lime, must be used to cement solid waste and produce backfilling materials of coal mines with a prescribed strength [9]. Nevertheless, the production of these binders is considered a serious contributor to occupational health hazards and life-threatening conditions [10,11]. Phosphogypsum could also bind waste byproducts [12], but the leaching of backfilling materials can release phosphates into the underground water [13]. Other binders, such as polymers and mechanically activated gangue powder, are energy consuming, and their production releases a huge amount of carbon dioxide into the atmosphere [14].

Hence, many researchers have been searching for new binders to tailor more environmentally friendly backfilling materials. This is the case of microbially induced carbonate precipitation (MICP), which is a more sustainable biomineralization technology [15–18], to be used as a novel binder. It is based on the enzymatic reaction of microorganisms that produce urease through cellular metabolism and catalyze the decomposition of urea to produce NH_4^+ and CO_3^{2-} ions, which, in turn, provide CO_3^{2-} for the mineralization reaction:



When calcium ions exist in the solution and meet the deposition conditions, CO_3^{2-} can be combined with them to form biological calcium carbonate of a certain crystal shape, according to the following reaction [19,20]:



The mechanism of microbial mineralization is shown in Figure 1 [21].

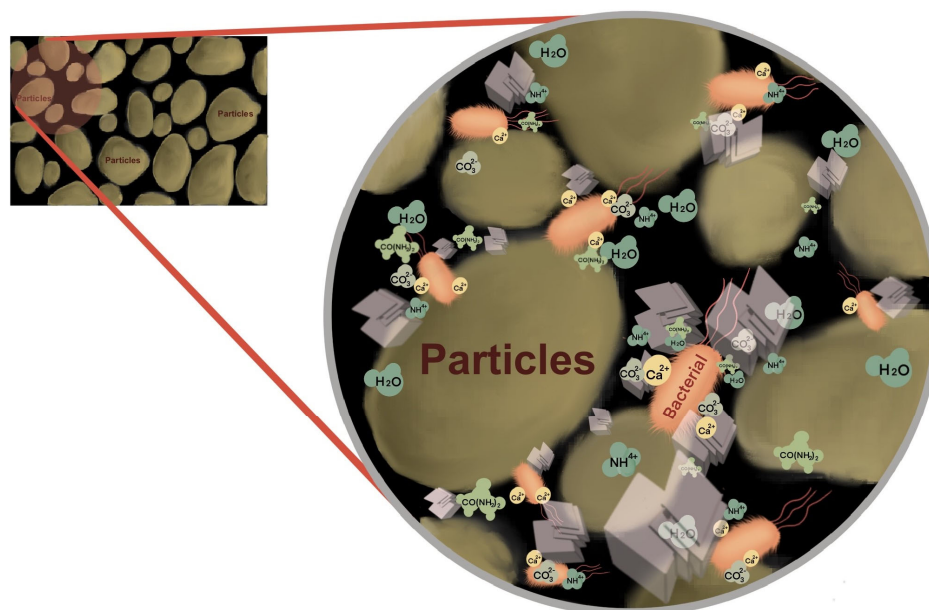


Figure 1. Mechanism of microbial mineralization.

This principle has great potential and good prospects to be developed in many applications. For example, to increase the durability and reduce the maintenance costs of concrete structures, micro-cracks can be continuously repaired by using MICP technology [22–24]. Some researchers studied the application of the MICP method to reinforce loose soils and improve the strength characteristics of expansive soils with low permeability [25–27]. In other studies, MICP technology reduced the release of heavy metals into the environment, because heavy metal ions can replace Ca^{2+} ions in the biocalcite structure [28–32].

In recent years, MICP technology has also been introduced in the field of backfilling. For example, microbial grouted sand was proposed by Deng et al. [33], and mineralized backfilling materials with bonding tailings were introduced by Liu et al. and Rong et al. [34].

While the versatility of MICP is evident in various applications, a significant gap in the current literature revolves around the micro-scale mineralization impact of solid waste on *B. pasteurii*. Existing studies have yet to comprehensively explore how different ingredients in backfill materials influence the mineralizing function of *B. pasteurii*. The recognition of the influence of backfill material ingredients on *B. pasteurii* mineralizing function could help enhancing material properties by making suitable changes.

Accordingly, the present study, devoted to the microbial mineralization of CG and FA, proposes a novel micro-scale view to understand the CG and FA impact on the *B. pasteurii* mineralizing function, and then, it is reflected in the material properties, in order to (1) reduce the environmental impact by substituting the traditional binders of backfilling materials in coal mines and (2) improve solid wastes handling by recycling CG and FA (i.e., CG and FA originating from the extraction and use of coal). Thus, in this paper, Section 2 reports the physical and chemical properties of CG and FA, and the preparation of bacterial strain and mineralized solutions. The experimental methods are given in Section 3. The experimental results, concerning the bacteria mineralizing function (micro-level) and then reflecting on properties of mineralized materials (macro-level) are analyzed and discussed in Section 4. Finally, the main findings of this study and ideas for future research are listed in Section 5.

2. Materials

Figure 2 shows the particle size distribution curves of CG (Figure 2a) and FA (Figure 2b), acquired using high-performance dry dispersion technology (Jinan Winner 3009B, Jinan Winner Particle Instrument Stock Co., Ltd., Jinan, China). CG was obtained by secondary sieving of natural CG from the Xinjulong coal mine, whereas FA was taken from Datang Henan power plant.

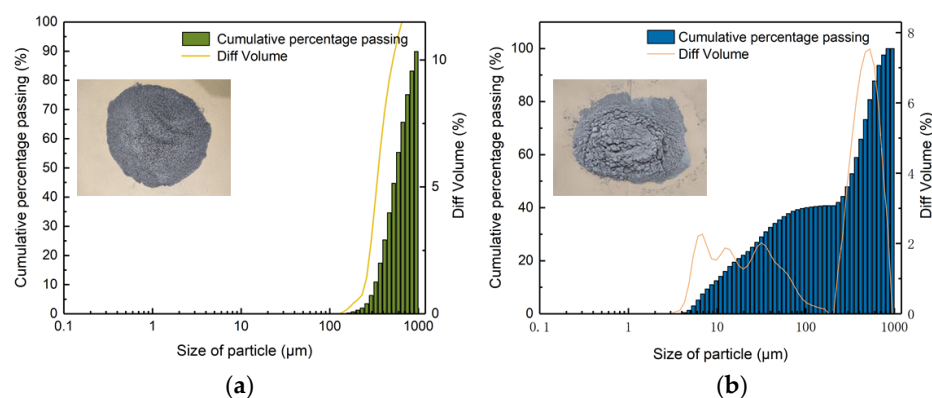


Figure 2. Particle size distribution of (a) CG and (b) FA.

Table 1 shows the chemical compositions of both CG and FA materials, which were measured at Jiangsu Design Institute of Geology for Mineral Resources (China) using the XRF technique. It can be observed that samples of CG and FA, which were dried, ground and sieved (through a 75- μm sieve) prior to analysis, are mainly composed of silicates, aluminates and other minor oxides.

Table 1. Chemical composition of CG and FA from XRF analysis.

Chemical Composition (%)	K ₂ O	Na ₂ O	SiO ₂	Al ₂ O ₃	Fe ₂ O ₃	CaO	MgO	TiO ₂	MnO ₂	P ₂ O ₅
Coal gangue	1.47	0.14	80.57	6.74	2.32	2.08	0.85	0.28	0.06	0.04
Fly ash	2.11	0.65	49.17	28.28	4.63	3.55	0.84	1.12	0.06	0.31

Bacillus pasteurii (*B. pasteurii*), herein employed as the target bacteria species, was obtained from Shaanxi Microbial Species Resource Conservation Center (China) with the

strain number A484. In a previous study [21], it was domesticated to be resistant to CG leaching solution and 1 M urea solution simultaneously. The basic culture medium was composed of 5 g/L tryptone, 3 g/L beef extract, a buffer regulator (0.42 g/L NaHCO₃ and 0.53g/L Na₂CO₃), deionized water and a certain amount of KOH to obtain a pH of 8.5. All mediums and equipment involved in the basic bacterial culture process were sterilized at 121 °C for 30 min [35].

B. pasteurii was firstly moved from the agar slant into the culture medium with an inoculating needle, and then incubated at 30 °C in a shaker, rotating at 120 rpm for 18 h, to obtain the seed cultivation. Afterwards, the seed cultivation was placed into the basic culture medium at a ratio of 2% *v/v*, and then in a constant temperature (at 30 °C) shaker (rotating at 150 rpm), followed by incubation. After 24 h, the strain matured, and the bacterial cultures derived from our custom research procedure were used for subsequent experiments.

Two mineralizing solutions, made with CaCl₂ and urea, respectively, were used in this study. CaCl₂ was autoclaved, whereas urea was filtrated with a 0.22 µm microporous filter membrane. The final concentration of both CaCl₂ and urea solutions was 0.5 M [36].

3. Methods

The mineralization function of *B. pasteurii* is the key factor to successfully prepare environmentally friendly backfilling materials. Unlike conventional binders, *B. pasteurii* is a living organism and environmentally sensitive. Therefore, it is important to understand, at a microscopic level, how CG and FA will affect the function of *B. pasteurii* and whether it can be used as a binder. When these microscopic behaviors are known, CG and FA can be suitably combined and used to cast the backfilling material for macroscopic tests.

3.1. Micro-Tests after the Addition of *B. pasteurii* to CG and FA

To discover the effect of CG and FA environments on the mineralizing capacity of *B. pasteurii* at the micro-level, they were added separately to the basic culture medium in two different tubes, also containing urea. The tubes, named FA group₁ and CG group₂, respectively, were placed in a shaker at a constant temperature of 30 °C. In this shaker, a third tube, considered as reference group₀, was also present. It contained the same basic culture medium of *B. pasteurii* and the same amount of urea, but without the presence of CG and FA. The compositions of the three groups used for micro-tests are shown in Table 2. From each tube, a 0.3 mL sample was extracted seven times (after 0 h, 6 h, 12 h, 24 h, 36 h, 48 h and 60 h) to be immediately subjected to a bacterial concentration test and a urea hydrolysis test. This procedure was repeated three times.

Table 2. Compositions of the three groups for micro-tests.

Components	Reference_0	FA Group_1	CG Group_2
CG (g)	0	0	1
FA (g)	0	1	0
Culture medium (mL)	5	5	5
<i>B. pasteurii</i> (mL)	0.1	0.1	0.1

The optical density (OD) test, based on the turbidity of the culture, was used to measure the *B. pasteurii* biomass concentration. Monitoring bacterial growth dynamics is routinely performed in a wide range of areas, and due to its relative ease of implementation, the OD measurement is widely adopted for this purpose. By utilizing the OD method, bacterial concentrations are approximated indirectly through changes in light scattering within the sample [37]. This approach provides real-time data on bacterial density, enhancing the utility of *B. pasteurii* across various industrial contexts. The maximum absorption peak (at λ = 645 nm) was obtained by full wavelength scanning [38] of *B. pasteurii* in a basic culture medium using a spectrophotometer (Puxi, China). A blank (uninoculated culture

medium) was used to calibrate the spectrophotometer prior to measuring the OD of the three groups. Subsequently, 0.3 mL was taken from the bacterial culture and transferred into a 10 mm cuvette to undergo a tenfold dilution. Finally, the density was measured with the above-mentioned spectrophotometer.

After adding urea to each group, conductivity tests, performed by means of a conductivity meter (Thermo Scientific Orion 410C-06A, Thermo Scientific, Waltham, MA, USA), detected when the *B. pasteurii* was producing urease (i.e., hydrolyzing urea and providing CO_3^{2-}) to be used in the subsequent mineralization reactions.

Inside the tubes, a precipitation generation experiment was carried out to exclude conductivity increases due to other factors or experimental errors, as well as to provide a multifaceted view of the mineralization phenomenon. A pre-test was first conducted to check whether a visible precipitation occurs immediately after the addition of CaCl_2 at a later stage of incubation (at least after 36 h). Accordingly, to clearly and visually observe the onset of mineralization of *B. pasteurii* in the CG and FA groups, respectively, CaCl_2 was added at different times (chosen according to the results of the urea hydrolysis test).

The precipitation samples were observed at various magnification levels using scanning electron microscopy (SEM; Sigma series; Zeiss, Jena, Germany). A thin layer of gold was sprayed on the samples to increase the electrical conductivity. In addition to SEM, energy-dispersive X-ray spectroscopy (EDS; X-Max 20; Oxford Instruments, Oxfordshire, UK) was used to identify the chemical elements of the samples.

To determine the presence of biominerals in the precipitation samples, a Bruker Vertex 80 V spectrophotometer was used to record the FTIR spectra (with the wavenumber ranging from 4000 to 400 cm^{-1}). Prior to analysis, precipitation materials were ground and mixed with 100 mg of KBr in an agate mortar under an infrared lamp, and then, the powder was pressed into transparent tablets with an infrared tablet press (YP-12).

As the different results from the previous test could be ascribed to the microscopic differences between CG and FA solid surfaces, the surface morphology of CG and FA was also observed and compared using SEM and optical microscopy (Leica DM500, Leica Microsystems, Wetzlar and Mannheim, Germany).

Through all these microscopic tests, it was possible to ascertain whether *B. pasteurii* plays a mineralizing role and whether it can be used as a binder in CG and FA systems.

3.2. Macro-Test on Backfilling Material

Two mortar mixtures, one containing only CG and *B. pasteurii* (in a solution of mass equal to 20% of the total) and one with FA, CG (with the mass ratio $\text{FA/CG} = 30\%$) and *B. pasteurii* (with the same mass solution of 20%), were prepared simultaneously under the same conditions. The compositions of the two mortars, named, respectively, A-spread and B-spread, are shown in Table 3. In the assessment of workability, the mortar spread was measured after 10 s (initial spread) because, depending on this value, the mortar can have either a good pumping performance (when the initial spread is ≥ 220 mm) or an excellent pumping performance (when it is ≥ 260 mm) [39,40].

To measure the strength of the new mortars at 28 days, another two mixtures containing both CG and FA (with a mass ratio $\text{FA/CG} = 30\%$), one mineralized by *B. pasteurii* (in a solution of mass equal to 20% of the total, named B-strength) and the other without *B. pasteurii* (named C-strength), were prepared under the same conditions (see Table 3). Afterwards, three samples for each mixture were cast in plastic cylindrical molds with an inner diameter of 50 mm and a length of 100 mm. After 1 day, the molds were removed, and the specimens were stored in a curing room at $30\text{ }^\circ\text{C}$ ($\text{RH} = 50\%$) for 28 days before performing the unconfined uniaxial compression test (UCT). According to the methods suggested by the Chinese National Standards for Geotechnical Testing (GB/T 50123–2019, GB/T 23561–2009) [41,42], the UCT was conducted by applying a compressive load which progressively increases at a speed of 1 mm/min. The UCT was performed three times for each mortar.

Table 3. Composition of the mortars used for macro-tests.

Components	A—Spread	B—Spread	B—Strength	C—Strength
CG (g)	2000	2000	1200	1200
FA (g)	0	600	360	360
<i>B. pasteurii</i> with mineralized solutions (mL)	500	650	390	0
Water (mL)	0	0	0	390

4. Results and Discussion

4.1. Micro-Tests after the Addition of *B. pasteurii* to CG and FA

4.1.1. Bacterial Concentration Test

In Figure 3, the curves of absorbance (ABS) of FA group_1 and CG group_2 are similar to that of Reference_0, as ABS increases according to the stages of the *B. pasteurii* growth curve. Each ABS vs. time curve shows almost the same three distinct phases: a short lag phase, a very rapid period of cell growth (exponential phase) and a maximum stationary phase, which continued until the 60th hour (60 h was the time of observation) [43,44].

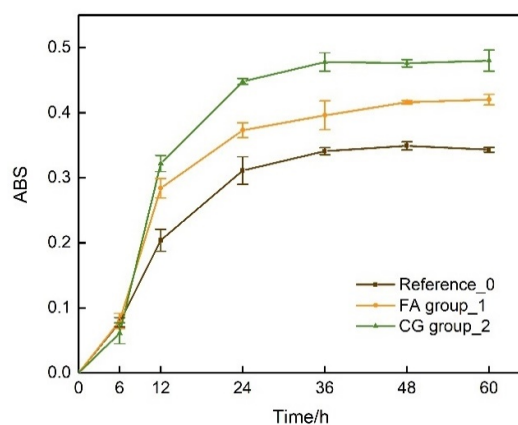


Figure 3. Effect of CG and FA environments on the biomass of *B. pasteurii*. The bacteria were cultivated in tubes and incubated for 60 h. FA group_1 and CG group_2 comprised *B. pasteurii* cultivated in basic culture medium with FA and CG, respectively. Reference_0 was composed of *B. pasteurii* cultivated in basic culture medium only. All of the tests were performed in triplicate. The vertical error bars indicate the standard deviation.

With respect to Reference_0, both FA group_1 and CG group_2 had a higher ABS, while the ABS in CG group_2 was the highest. This indicates that the addition of *B. pasteurii* to CG and FA does not affect the normal growth of *B. pasteurii*, and a significant increment in biomass was observed in the two groups. Indeed, bacteria in a liquid environment tend to adhere to solid surfaces for growth, which fosters their multiplication and anticipates the beginning of biological processes [45,46], such as that given in Equation (1). Thus, CG and FA culturing conditions can enhance the biomass of *B. pasteurii*, especially when it is an important factor influencing the mineralization performance.

4.1.2. Urea Hydrolysis Test

As is shown in Figure 4, the conductivity increases in all three groups of Table 2. In fact, the urease reaction involves the hydrolysis of the non-ionic substrate urea and, also in the absence of calcium ions, generates the NH_4^+ and CO_3^{2-} ionic products. As a result, the corresponding increment in the electrical conductivity of the liquid can be measured [47]. At the same time, higher concentrations of ammonia produced from urea facilitate the production of adenosine triphosphate by ureolytic bacteria, speed up the metabolism and increase enzyme activity [48]. As the incubation time increases, *B. pasteurii* hydrolyzes

more urea, thus producing and accumulating more ions and increasing the conductivity of the liquid more rapidly.

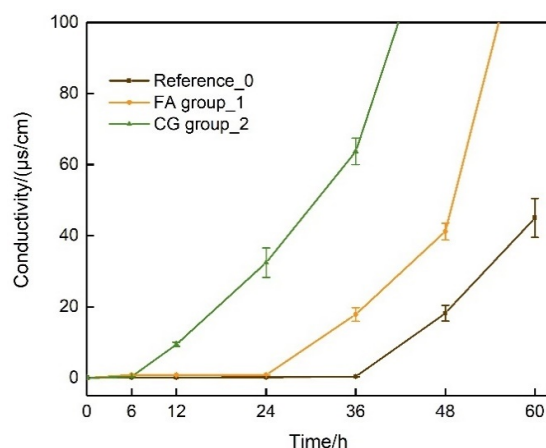


Figure 4. Effect of CG and FA environments on the conductivity of *B. pasteurii* cultures. The bacteria were cultivated in tubes and incubated for 60 h. The experimental groups were composed of *B. pasteurii* cultivated in basic culture medium and urea with CG and FA, respectively. Reference_0 comprised *B. pasteurii* cultivated in basic culture medium and urea. Each set of data is displayed as the difference from the 0 h data. All tests were performed in triplicate and the vertical error bars indicate the standard deviation.

It was noted that the mineralization began to occur after approximately 12 h, 31 h and 43 h in CG group_2, FA group_1 and Reference_0, respectively. As the addition of *B. pasteurii* to CG resulted in mineralization occurring 31 h earlier than that in Reference_0, it is possible to reduce the time when biomineralization begins to occur by approximately 72%, with respect to the systems without CG or FA. Likewise, the addition of *B. pasteurii* to FA resulted in mineralization occurring 12 h earlier than that in the control group, which could decrease the time at which biomineralization begins by only 28%. In other words, the coexistence of CG (or FA) with *B. pasteurii* not only facilitates *B. pasteurii* multiplication but also boosts the production of urease by *B. pasteurii*, enabling a faster start to urea hydrolysis compared to the original culture method. Thus, with the addition of CG (or FA), the initiation of the MICP reaction process is accelerated.

4.1.3. In Situ Urea Hydrolysis Experiment

After the production of CO_3^{2-} due to the *B. pasteurii* hydrolysis of urea (see Section 4.1.2), additional calcium chloride solution was added for the in situ test, which was conducted at three specific time points: 12 h, 36 h and 48 h. As also observed by other researchers [49,50], the white bioprecipitate, shown in Figure 5a, formed immediately. This precipitate was used to assess whether the mineralization had occurred in the culturing system after incubating the bacteria within urea and, subsequently, adding calcium chloride.

Based on the results of the conductivity tests (see Figure 4), in situ urea hydrolysis tests were also carried out. In particular, Figure 5 shows the comparison between the tubes containing CG group_2, FA group_1 and Reference_0 after 12 h (Figure 5b), 36 h (Figure 5c) and 48 h (Figure 5d) of urea hydrolysis, respectively. If precipitation occurred after the addition of CaCl_2 , then the bacteria within the solution performed mineralization and generated CO_3^{2-} [51].

As illustrated on the left side of Figure 5b, the addition of CaCl_2 after 12 h resulted in a bioprecipitate in the tube containing CG group_2. Thus, CO_3^{2-} was present in this solution, and *B. pasteurii* were able to perform mineralization. In the other two groups (see the tubes on the right side of Figure 5b), precipitation did not occur immediately, indicating that no CO_3^{2-} was present at this time and that the urea was not hydrolyzed by *B. pasteurii*.

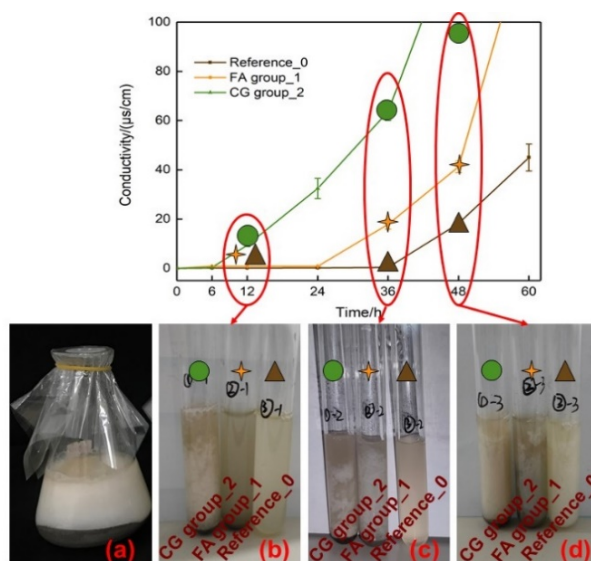


Figure 5. (a) A pre-test: Mineralization occurring from a macroscopic perspective. After the introduction of calcium ions, a white bioprecipitate was formed immediately. (b–d) Phenomena after the simultaneous addition of CaCl_2 solution to three sets of test tubes at the 12 h, 36 h and 48 h incubation time points (from left to right), respectively. The test tubes comprise CG group_2, FA group_1 and Reference_0. Different symbols correspond to different test tubes.

The addition of CaCl_2 to the three groups after 36 h (Figure 5c) immediately produced white precipitates in the two tubes on the left side (CG group_2 and FA group_1), indicating that *B. pasteurii* in the solution were already performing the mineralization function and secreting urease to hydrolyze the urea contained in these tubes. At this time, as in the previous case, mineralization by the bacteria did not commence in Reference_0 (the tube on the right side of Figure 5c did not show any precipitation). Finally, when CaCl_2 was added at 48 h (Figure 5d), bioprecipitation occurred in all tubes. Therefore, at this time, the bacteria were performing their mineralization function in all three groups.

The previous tests demonstrate that the addition of bacteria to CG or FA does not inhibit the mineralization of the bacteria, but rather, it shortens the initiation time. Indeed, the bacteria in Reference_0 took the longest time to develop their mineralization function, whereas in CG group_2, they can perform their mineralization function earlier than in FA group_1. Moreover, the results of this macroscopic analysis are consistent with those of the microscopic urea hydrolysis tests described in Section 4.1.2.

4.1.4. SEM/EDS and FTIR Precipitation Test

All of the biochemical reaction products under *B. pasteurii* mineralization were also investigated by means of SEM/EDS and FTIR, in order to analyze their morphology and composition.

In Figure 6a,b, the structure of the bioprecipitate can be clearly observed using SEM at different magnifications, indicating that plate-like layers were stacked to form ellipsoids. A similar morphology was also observed in other studies [52–54]. A clear rod-shaped bacterial structure (a typical shape of *B. pasteurii*) of diameter 0.5–1.5 μm , which is consistent with other researchers [55], along with calcite crystals, can also be observed in Figure 6a. Thus, during the mineralization process, bacteria functioned as nucleation sites [56]. The presence of *Bacillus* species surrounded by mineralization products was described in detail by Sharma et al. [57]. Finally, EDS quantification revealed that the elemental composition of the bioprecipitate shown in Figure 6c was mostly calcium, carbon and oxygen (see Figure 6d).

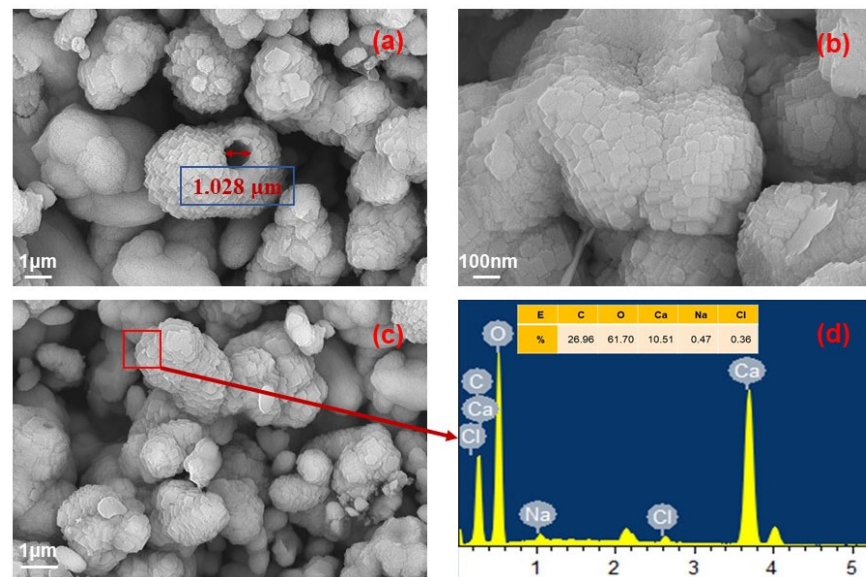


Figure 6. Scanning electron microscopy images of the bioprecipitate (a) at 7500 times magnification and (b) at 20,000 times magnification. (c) SEM image and (d) EDS analysis of the bioprecipitate. EDS data are shown from one of several determinations (abscissa unit: keV).

In Figure 7, strong absorption bands were observed at 875 cm^{-1} and approximately 1414 cm^{-1} , which is consistent with other researchers [58,59]. They belong to the C–O bond characteristic of CaCO_3 , mainly present in CG group_1 and FA group_2, and confirm the MICP process. These characteristic peaks are not present in only FA (Figure 7b). Although very small vibrational bands were also present in only CG (Figure 7a), this suggests that the latter contains very low levels of carbonate derived from natural chemical processes. The absorption located at around 795 cm^{-1} is assigned to Si–O stretching vibrations, which suggests the presence of quartz in CG (Figure 7a) and FA (Figure 7b). It must be remarked that the results of FTIR spectroscopy were consistent with those of both the SEM/EDS analyses and the MICP process.

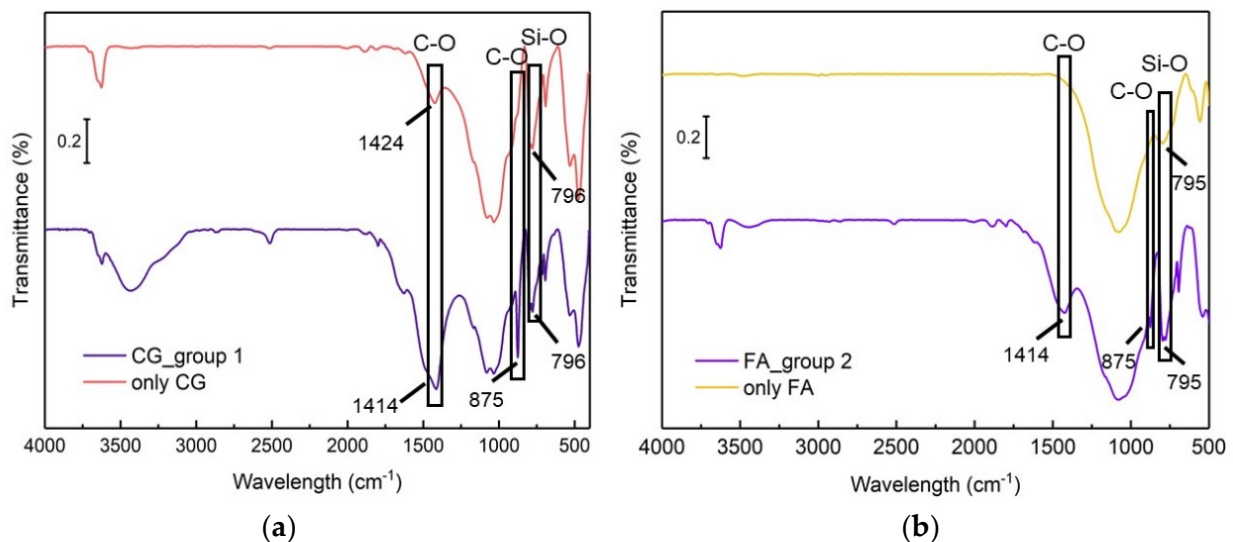


Figure 7. FTIR spectra of (a) the bioprecipitate in the CG group compared with only CG and of (b) the bioprecipitate in the FA group compared with only FA. A small amount of CG or FA substrate is mixed in the bioprecipitate.

4.1.5. Effect of Solid Surface Roughness on *B. pasteurii*

SEM and OM images (Figure 8) showed different sizes among CG, FA and *B. pasteurii*. As can be seen in Figure 8a,b, CG is much larger compared to FA. In order to observe *B. pasteurii* clearly and compare its size with FA, OM is used (Figure 8c,d). And it shows that the size of *B. pasteurii* is close to some FA particles. Therefore, the *B. pasteurii* we selected has a size comparable with that of FA, whereas CG has the largest size.

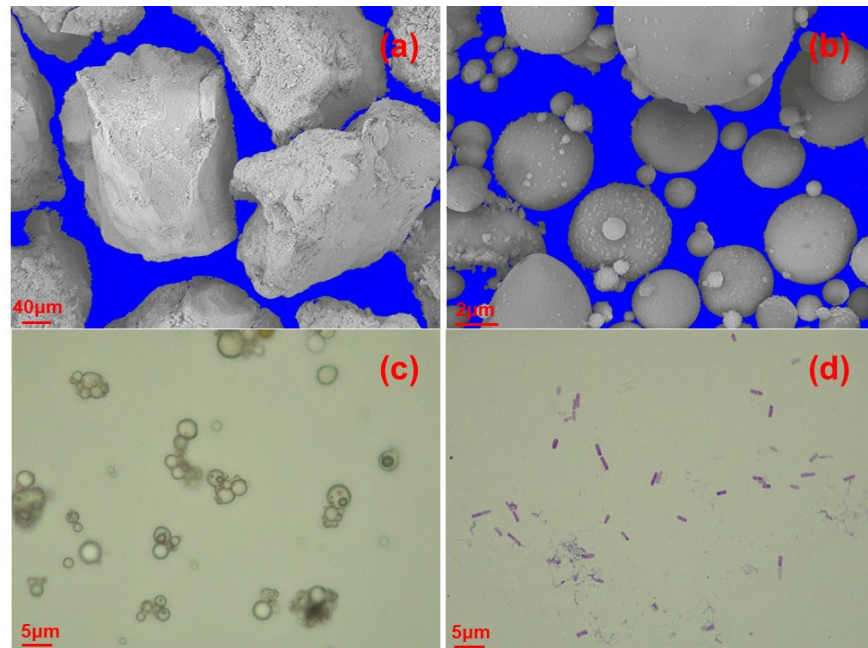


Figure 8. (a) Image of CG particles (magnified 200 times) and (b) SEM of FA particles (magnified 5000 times). OM images of (c) FA magnified 1000 times and (d) *B. pasteurii* magnified 1000 times. A typical image is taken from many similar examples.

In Figure 9, the CG particles have a rough surface, whereas most of the FA has a smooth surface. Surface roughness is a major factor affecting adhesion [60], because if the surface is smooth and the spacing between the filaments is smaller than the size of the bacteria, the adhesion of bacteria is reduced [61]. With a larger anchoring area, bacterial adhesion of the rough surface can be enhanced. Hence, it is easier for *B. pasteurii* to adhere to the CG surface (Figure 9a). In other words, the presence of CG promotes, more than FA (Figure 9b), the *B. pasteurii* adhesion and growth. The microorganisms in the system are able to reach a stable growth phase and start their biological processes more rapidly [62]. For this reason, the CG environment contains a greater *B. pasteurii* biomass to hydrolyze urea, resulting in a faster increase in conductivity than in FA. As a consequence, mineralization occurs in a short time.

4.2. Macro-Test on the Backfilling Material

Spread was measured in order to quantify the workability of the mortars described in Section 3.2 (see Figure 10a and Table 4). As is shown in Figure 10b, there is no workability in the mortar without FA (A-spread). On the contrary, B-spread, which contained CG, 30% FA and *B. pasteurii* with mineralized solutions, showed good pumping performances, as the initial average spread was 243 mm (Figure 10c).

Table 4. Average properties of the backfilling material macro-test.

Mortar	Compressive Strength (KPa)	Spread after 10 s (mm)
A	/	100
B	471	243
C	88.22	/

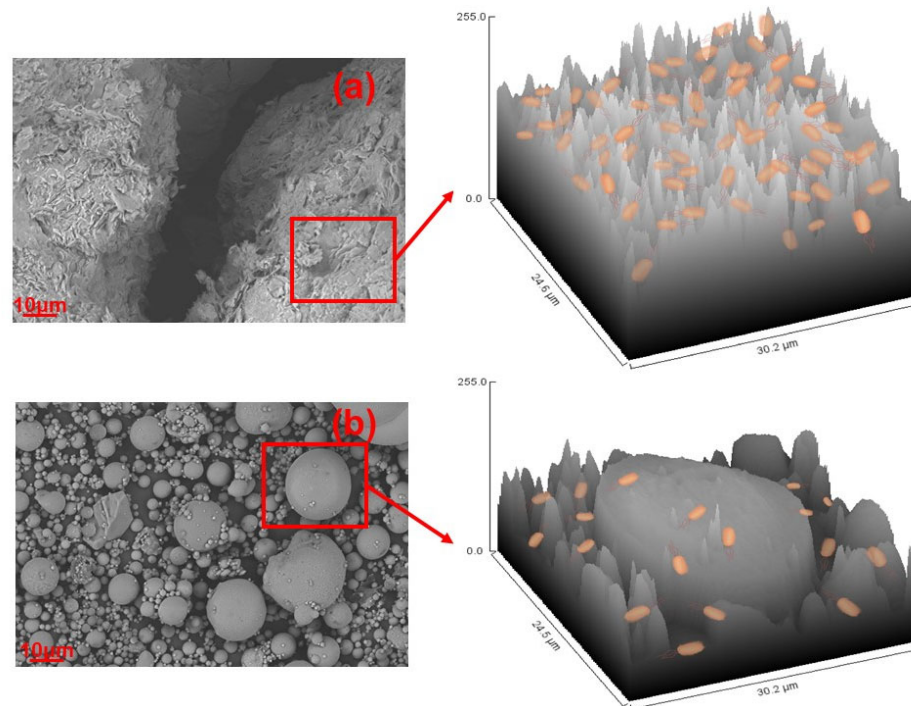


Figure 9. SEM (magnified 1000 times) of (a) CG with its surface plot and (b) FA with its surface plot. Schematic diagram of *B. pasteurii* adhesion is shown on different rough surfaces and anchoring areas. A typical image is taken from many similar examples.

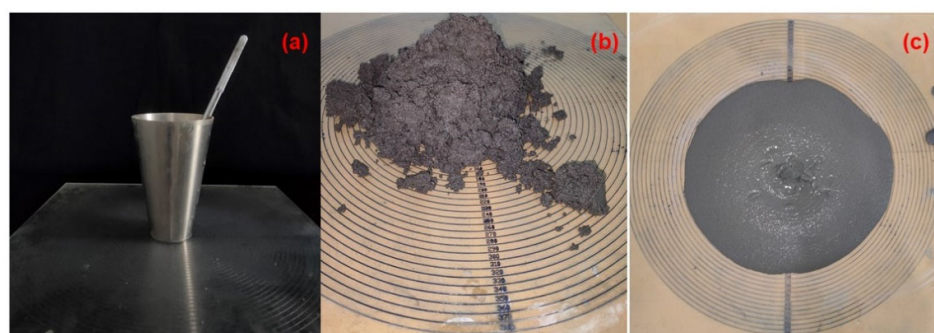


Figure 10. Mortar spread tests. (a) Spread testing bucket; (b) A-spread: mortar without FA; (c) B-spread: mortar with CG, 30% FA and *B. pasteurii* with mineralized solutions.

Due to the microbial mineralization of CG and FA, the average compressive strength of the mortar B-strength reached 0.471 MPa (refer to Section 3.2 for detailed strength measurement procedures, see Table 4 and Figure 11a), which is higher than the value of 0.0882 MPa measured in the C-strength group of CG and FA materials only (Figure 11b). Therefore, the addition of *B. pasteurii* to CG and FA aggregates for mineralization can increase the strength of the material by approximately 5.34 times. In other words, in B-strength mortar, microorganisms can not only survive in the presence of CG and FA but also effectively perform the mineralization function.

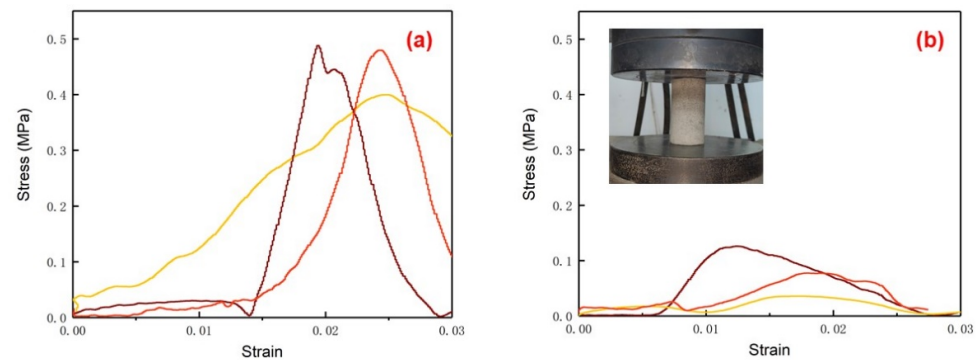


Figure 11. Results of the compression test on (a) B-strength: microbially mineralized solid waste CG and FA materials; and (b) C-strength: microbial-free original solid CG and FA.

Combined with the results of rheology tests, we can argue that the backfilling material prepared by microbially mineralized CG and FA not only has the mechanical performance to play the role of a green binder, but its slurry also has excellent pumping properties. Therefore, based on the effect of CG and FA on the mineralizing capacity of *B. pasteurii* at the micro-level, CG and FA could be accepted well as substrates for biomineralized composites to be used as backfilling materials. Accordingly, the present study also gives new insights into biomineralization in backfill materials and contributes to the sustainable development of the environment by utilizing solid waste in an effective way and reducing the risk of hazardous materials.

5. Conclusions

Beginning with micro-level tests on bacteria co-cultured with CG and FA, and ending with macro-tests on mortars made with CG, FA and bacteria, the conclusions of this paper are as follows:

- Both CG and FA environments are favorable for the growth of *B. pasteurii*.
- CG and FA environments can significantly shorten the initiation time for urea hydrolysis and mineralization. The time for the occurrence of *B. pasteurii* mineralization is reduced by 72% when using CG and by 28% in the presence of FA.
- A reason why *B. pasteurii* performs better in the CG environment than in FA may be ascribed to the substrate surface roughness, which offers more attachment sites.
- SEM and FTIR analyses confirmed that the mineralization precipitate, generated by the co-culture of *B. pasteurii* with CG or FA, is bio- CaCO_3 .
- Mortars with CG, 30% FA and *B. pasteurii* with mineralized solutions showed a better pumping performance than in the absence of FA.
- The compressive strength of biomineralized materials at 28 days is 5.34 times higher than that obtained without biomineralizing.
- Finally, our findings support the viability of using microbial mineralized coal gangue and fly ash for eco-friendly backfilling materials, demonstrating potential benefits for sustainable practices in coal mining operations.

As this is the first study on the effect of CG and FA on the mineralizing capacity of *B. pasteurii*, future research will be devoted to accelerating *B. pasteurii* mineralization and improving the strength of the backfilling material. Moreover, the use of other solid wastes, with a rougher surface, will also be investigated.

Author Contributions: S.G.: Conceptualization, Methodology, Writing—Original Draft. A.P.F.: Supervision, Writing—Review and Editing. H.Y.: Writing—Review and Editing. K.S.: Validation. L.D.: Validation. All authors have read and agreed to the published version of the manuscript.

Funding: This research was funded by the China Scholarship Council (CSC, No.202106420067), the future scientists Program of China University of Mining and Technology (2021WLKXJ018) and the Postgraduate Research & Practice Innovation Program of Jiangsu Province (KYCX21_2336).

Institutional Review Board Statement: Not applicable.

Informed Consent Statement: Not applicable.

Data Availability Statement: Data is contained within the article.

Acknowledgments: We are grateful to China University of Mining and Technology for providing us with the experimental platform.

Conflicts of Interest: The authors declare no conflict of interest.

References

1. Djamaluddin, I.; Mitani, Y.; Esaki, T. Evaluation of ground movement and damage to structures from Chinese coal mining using a new GIS coupling model. *Int. J. Rock Mech. Min. Sci.* **2011**, *48*, 380–393. [[CrossRef](#)]
2. Pandey, V.C. Direct seeding offers affordable restoration for fly ash deposits. *Energy Ecol. Environ.* **2022**, *7*, 453–460. [[CrossRef](#)]
3. Zierold, K.M.; Odoh, C. A review on fly ash from coal-fired power plants: Chemical composition, regulations, and health evidence. *Rev. Environ. Health* **2020**, *35*, 401–418. [[CrossRef](#)]
4. Yakun, S.; Xingmin, M.; Kairong, L.; Hongbo, S. Soil characterization and differential patterns of heavy metal accumulation in woody plants grown in coal gangue wastelands in Shaanxi, China. *Environ. Sci. Pollut. Res.* **2016**, *23*, 13489–13497. [[CrossRef](#)] [[PubMed](#)]
5. Cavusoglu, I.; Yilmaz, E.; Yilmaz, A.O. Sodium silicate effect on setting properties, strength behavior and microstructure of cemented coal fly ash backfill. *Powder Technol.* **2021**, *384*, 17–28. [[CrossRef](#)]
6. Du, X.; Feng, G.; Qi, T.; Guo, Y.; Zhang, Y.; Wang, Z. Failure characteristics of large unconfined cemented gangue backfill structure in partial backfill mining. *Constr. Build. Mater.* **2019**, *194*, 257–265. [[CrossRef](#)]
7. Liu, H.; Zhang, J.; Li, B.; Zhou, N.; Xiao, X.; Li, M.; Zhu, C. Environmental behavior of construction and demolition waste as recycled aggregates for backfilling in mines: Leaching toxicity and surface subsidence studies. *J. Hazard. Mater.* **2020**, *389*, 121870. [[CrossRef](#)] [[PubMed](#)]
8. Bharathan, B.; McGuinness, M.; Kuhar, S.; Kermani, M.; Hassani, F.P.; Sasmito, A.P. Pressure loss and friction factor in non-Newtonian mine paste backfill: Modelling, loop test and mine field data. *Powder Technol.* **2019**, *344*, 443–453. [[CrossRef](#)]
9. Zhou, N.; Zhang, J.; Ouyang, S.; Deng, X.; Dong, C.; Du, E. Feasibility study and performance optimization of sand-based cemented paste backfill materials. *J. Clean. Prod.* **2020**, *259*, 120798. [[CrossRef](#)]
10. Li, B.; Ju, F. An experimental investigation into the compaction characteristic of granulated gangue backfilling materials modified with binders. *Environ. Earth. Sci.* **2018**, *77*, 1–9. [[CrossRef](#)]
11. Etim, M.-A.; Babaremu, K.; Lazarus, J.; Omole, D. Health risk and environmental assessment of cement production in Nigeria. *Atmosphere* **2021**, *12*, 1111. [[CrossRef](#)]
12. Calderón-Morales, B.R.; García-Martínez, A.; Pineda, P.; García-Tenório, R. Valorization of phosphogypsum in cement-based materials: Limits and potential in eco-efficient construction. *J. Build. Eng.* **2021**, *44*, 102506. [[CrossRef](#)]
13. Shi, Y.; Cheng, L.; Tao, M.; Tong, S.; Yao, X.; Liu, Y. Using modified quartz sand for phosphate pollution control in cemented phosphogypsum (PG) backfill. *J. Clean. Prod.* **2021**, *283*, 124652. [[CrossRef](#)]
14. Yu, C.; Zhang, L.; Zheng, D.; Yang, F.; Wang, Q.; Wu, W.; Wang, C.; Cang, D. Research progress of geopolymer materials prepared from solid waste and their applications. *Sci. Sin. Tech.* **2022**, *52*, 529–546. [[CrossRef](#)]
15. Tian, Z.; Tang, X.; Xiu, Z.; Zhou, H.; Xue, Z. The mechanical properties improvement of environmentally friendly fly ash-based geopolymer mortar using bio-mineralization. *J. Clean. Prod.* **2022**, *332*, 130020. [[CrossRef](#)]
16. Karimian, A.; Hassanlourad, M. Mechanical behaviour of MICP-treated silty sand. *Bull. Eng. Geol. Environ.* **2022**, *81*, 285. [[CrossRef](#)]
17. Farhadi, S.; Ziadloo, S. Self-healing microbial concrete—A review. In *Materials Science Forum*; Trans Tech Publications Ltd.: Stafa-Zurich, Switzerland, 2020; pp. 8–12. [[CrossRef](#)]
18. Proudfoot, D.; Brooks, L.; Gammons, C.H.; Barth, E.; Bless, D.; Nagisetty, R.M.; Lauchnor, E.G. Investigating the potential for microbially induced carbonate precipitation to treat mine waste. *J. Hazard. Mater.* **2022**, *424*, 127490. [[CrossRef](#)] [[PubMed](#)]
19. Cheng, L.; Shahin, M.A. Microbially induced calcite precipitation (MICP) for soil stabilization. In *Ecological Wisdom Inspired Restoration Engineering*; Springer: Singapore, 2019; pp. 47–68. [[CrossRef](#)]
20. Li, M.; Zhu, X.; Mukherjee, A.; Huang, M.; Achal, V. Biomineralization in metakaolin modified cement mortar to improve its strength with lowered cement content. *J. Hazard. Mater.* **2017**, *329*, 178–184. [[CrossRef](#)] [[PubMed](#)]
21. Guo, S.; Zhang, J.; Li, M.; Zhou, N.; Song, W.; Wang, Z.; Qi, S. A preliminary study of solid-waste coal gangue based biomineralization as eco-friendly underground backfill material: Material preparation and macro-micro analyses. *Sci. Total Environ.* **2021**, *770*, 145241. [[CrossRef](#)]
22. Yu, X.; He, Z.; Li, X. Bio-cement-modified construction materials and their performances. *Environ. Sci. Pollut. Res.* **2022**, *29*, 11219–11231. [[CrossRef](#)]
23. Nasser, A.A.; Sorour, N.M.; Saafan, M.A.; Abbas, R.N. Microbially-Induced-Calcite-Precipitation (MICP): A biotechnological approach to enhance the durability of concrete using *Bacillus pasteurii* and *Bacillus sphaericus*. *Heliyon* **2022**, *8*, e09879. [[CrossRef](#)] [[PubMed](#)]

24. Van Wylick, A.; Monclaro, A.V.; Elsacker, E.; Vandelook, S.; Rahier, H.; De Laet, L.; David, C.; Peeters, E. A review on the potential of filamentous fungi for microbial self-healing of concrete. *Fungal Biol. Biotechnol.* **2021**, *8*, 16. [[CrossRef](#)] [[PubMed](#)]
25. Gowthaman, S.; Nakashima, K.; Kawasaki, S. Freeze-thaw durability and shear responses of cemented slope soil treated by microbial induced carbonate precipitation. *Soils Found.* **2020**, *60*, 840–855. [[CrossRef](#)]
26. Tang, X.; Chen, L.; Zhang, G.; Jiang, P. Research and Application of Microbial Cement in Civil Engineering. *J. Simul.* **2022**, *10*, 35.
27. Zeng, C.; Veenis, Y.; Hall, C.A.; Young, E.S.; van Der Star, W.R.; Zheng, J.J.; Van Paassen, L.A. Experimental and numerical analysis of a field trial application of microbially induced calcite precipitation for ground stabilization. *J. Geotech. Geoenviron. Eng.* **2021**, *147*, 05021003. [[CrossRef](#)]
28. Song, H.; Kumar, A.; Ding, Y.; Wang, J.; Zhang, Y. Removal of Cd²⁺ from wastewater by microorganism induced carbonate precipitation (MICP): An economic bioremediation approach. *Sep. Purif. Technol.* **2022**, *297*, 121540. [[CrossRef](#)]
29. Wang, M.; Wu, S.; Guo, J.; Zhang, X.; Yang, Y.; Chen, F.; Zhu, R. Immobilization of cadmium by hydroxyapatite converted from microbial precipitated calcite. *J. Hazard. Mater.* **2019**, *366*, 684–693. [[CrossRef](#)] [[PubMed](#)]
30. Song, J.; Han, B.; Song, H.; Yang, J.; Zhang, L.; Ning, P.; Lin, Z. Nonreductive biomineralization of uranium by *Bacillus subtilis* ATCC-6633 under aerobic conditions. *J. Environ. Radioact.* **2019**, *208*, 106027. [[CrossRef](#)]
31. Zeng, Y.; Chen, Z.; Lyu, Q.; Cheng, Y.; Huan, C.; Jiang, X.; Yan, Z.; Tan, Z. Microbiologically induced calcite precipitation for in situ stabilization of heavy metals contributes to land application of sewage sludge. *J. Hazard. Mater.* **2023**, *441*, 129866. [[CrossRef](#)]
32. Rajasekar, A.; Wilkinson, S.; Moy, C.K.S. MICP as a potential sustainable technique to treat or entrap contaminants in the natural environment: A review. *Environ. Sci. Ecotechnol.* **2021**, *6*, 100096. [[CrossRef](#)]
33. Deng, X.; Li, Y.; Wang, F.; Shi, X.; Yang, Y.; Xu, X.; Huang, Y.; de Wit, B. Experimental study on the mechanical properties and consolidation mechanism of microbial grouted backfill. *Int. J. Min. Sci. Technol.* **2022**, *32*, 271–282. [[CrossRef](#)]
34. Gui, R.; Pan, Y.-X.; Ding, D.-X.; Liu, Y.; Zhang, Z.-J. Experimental study on the fine-grained uranium tailings reinforced by MICP. *Adv. Civ. Eng.* **2018**, *2018*, 2928985. [[CrossRef](#)]
35. Pinheiro, V.E.; Michelin, M.; Vici, A.C.; de Almeida, P.Z.; Teixeira de Moraes Polizeli, M.d.L. *Trametes versicolor* laccase production using agricultural wastes: A comparative study in Erlenmeyer flasks, bioreactor and tray. *Bioprocess Biosyst. Eng.* **2020**, *43*, 507–514. [[CrossRef](#)]
36. Wang, Z.; Zhang, J.; Li, M.; Guo, S.; Zhang, J.; Zhu, G. Experimental study of microorganism-induced calcium carbonate precipitation to solidify coal gangue as backfill materials: Mechanical properties and microstructure. *Environ. Sci. Pollut. Res.* **2022**, *29*, 45774–45782. [[CrossRef](#)]
37. Yu, A.C.S.; Loo, J.F.C.; Yu, S.; Kong, S.K.; Chan, T.F. Monitoring bacterial growth using tunable resistive pulse sensing with a pore-based technique. *Appl. Microbiol. Biotechnol.* **2014**, *98*, 855–862. [[CrossRef](#)] [[PubMed](#)]
38. Wang, J.; Zhang, Q.; Chen, N.; Chen, J.; Zhou, J.; Li, J.; Wei, Y.; Bu, D. A new species of *Desmodesmus* sp. from high altitude area was discovered and its isolated, purification, amplification culture and species identification were studied. *Preprint* **2022**. [[CrossRef](#)]
39. An, H.; Fu, R.; Lu, Y.; Kong, D.; Luo, S.; Wang, L.; Lv, F. Effect of heat treatment time on splitting tensile properties of phosphogypsum-based composite cementitious materials. *Bull. Silic.* **2022**, *41*, 545–552. [[CrossRef](#)]
40. Yaseri, S.; Mahdikhani, M.; Jafarinoor, A.; Verki, V.M.; Esfandyari, M.; Ghiasian, S.M. The development of new empirical apparatuses for evaluation fresh properties of self-consolidating mortar: Theoretical and experimental study. *Constr. Build. Mater.* **2018**, *167*, 631–648. [[CrossRef](#)]
41. Committee, C.N.S. *Standard for Geotechnical Testing Method*; China Planning Press: Beijing, China, 2019.
42. Committee, C.N.S. *Methods for Determining the Physical and Mechanical Properties of Coal and Rock*; China Planning Press: Beijing, China, 2009.
43. Szalwinski, L.J.; Gonzalez, L.E.; Morato, N.M.; Marsh, B.M.; Cooks, R.G. Bacterial growth monitored by two-dimensional tandem mass spectrometry. *Analyst* **2022**, *147*, 940–946. [[CrossRef](#)]
44. Paulton, R.J. The bacterial growth curve. *J. Biol. Educ.* **1991**, *25*, 92–94. [[CrossRef](#)]
45. Garrett, T.R.; Bhakoo, M.; Zhang, Z. Bacterial adhesion and biofilms on surfaces. *Prog. Nat. Sci.* **2008**, *18*, 1049–1056. [[CrossRef](#)]
46. Zheng, S.; Bawazir, M.; Dhall, A.; Kim, H.-E.; He, L.; Heo, J.; Hwang, G. Implication of surface properties, bacterial motility, and hydrodynamic conditions on bacterial surface sensing and their initial adhesion. *Front. Bioeng. Biotechnol.* **2021**, *9*, 643722. [[CrossRef](#)] [[PubMed](#)]
47. Al-Thawadi, S. High Strength In-Situ Biocementation of Soil by Calcite Precipitating Locally Isolated Ureolytic Bacteria. Ph.D. Dissertation, Murdoch University, Perth, Australia, 2008. Available online: <https://researchrepository.murdoch.edu.au/id/eprint/721/> (accessed on 23 October 2023).
48. Mempin, R.; Tran, H.; Chen, C.; Gong, H.; Kim Ho, K.; Lu, S. Release of extracellular ATP by bacteria during growth. *BMC Microbiol* **2013**, *13*, 301. [[CrossRef](#)]
49. Harkes, M.P.; Van Paassen, L.A.; Booster, J.L.; Whiffin, V.S.; van Loosdrecht, M.C. Fixation and distribution of bacterial activity in sand to induce carbonate precipitation for ground reinforcement. *Ecol. Eng.* **2010**, *36*, 112–117. [[CrossRef](#)]
50. Yu, X.; Rong, H. Seawater based MICP cements two/one-phase cemented sand blocks. *Appl. Ocean Res.* **2022**, *118*, 102972. [[CrossRef](#)]
51. Gebru, K.A.; Kidanemariam, T.G.; Gebretinsae, H.K. Bio-cement production using microbially induced calcite precipitation (MICP) method: A review. *Chem. Eng. Sci.* **2021**, *238*, 116610. [[CrossRef](#)]

52. Zhao, J.; Dyer, T.; Csetenyi, L.; Jones, R.; Gadd, G.M. Fungal colonization and biomineralization for bioprotection of concrete. *J. Clean. Prod.* **2022**, *330*, 129793. [[CrossRef](#)]
53. Kang, B.; Zha, F.; Li, H.; Xu, L.; Sun, X.; Lu, Z. Bio-mediated method for immobilizing copper tailings sand contaminated with multiple heavy metals. *Crystals* **2022**, *12*, 522. [[CrossRef](#)]
54. Yao, D.; Wu, J.; Wang, G.; Wang, P.; Zheng, J.-J.; Yan, J.; Xu, L.; Yan, Y. Effect of wool fiber addition on the reinforcement of loose sands by microbially induced carbonate precipitation (MICP): Mechanical property and underlying mechanism. *Acta Geotech.* **2021**, *16*, 1401–1416. [[CrossRef](#)]
55. Rui, Y.; Qian, C. Characteristics of different bacteria and their induced biominerals. *J. Ind. Eng. Chem.* **2022**, *115*, 449–465. [[CrossRef](#)]
56. Zehner, J.; Røyne, A.; Sikorski, P. Calcite seed-assisted microbial induced carbonate precipitation (MICP). *PLoS ONE* **2021**, *16*, e0240763. [[CrossRef](#)] [[PubMed](#)]
57. Sharma, M.; Satyam, N.; Reddy, K.R. Investigation of various gram-positive bacteria for MICP in Narmada Sand, India. *Int. J. Geotech. Eng.* **2021**, *15*, 220–234. [[CrossRef](#)]
58. Zheng, T.; Hou, D.; Leng, W.; Li, P.; Wei, W. Preparation, characterization, and formation mechanism of different biological calcium carbonate (CaCO₃) induced by *Bacillus mucilaginosus* and *Bacillus alcalophilus*. *J. Nanopart. Res.* **2023**, *25*, 189. [[CrossRef](#)]
59. Feng, Z.; Li, X. Microbially induced calcite precipitation and synergistic mineralization cementation mechanism of Pisha sandstone components. *Sci. Total Environ.* **2023**, *866*, 161348. [[CrossRef](#)] [[PubMed](#)]
60. Yang, K.; Shi, J.; Wang, L.; Chen, Y.; Liang, C.; Yang, L.; Wang, L.-N. Bacterial anti-adhesion surface design: Surface patterning, roughness and wettability: A review. *J. Mater. Sci. Technol.* **2022**, *99*, 82–100. [[CrossRef](#)]
61. Encinas, N.; Yang, C.-Y.; Geyer, F.; Kaltbeitzel, A.; Baumli, P.; Reinholz, J.; Mailänder, V.; Butt, H.-J.R.; Vollmer, D. Submicrometer-sized roughness suppresses bacteria adhesion. *ACS Appl. Mater. Interfaces* **2020**, *12*, 21192–21200. [[CrossRef](#)]
62. Carniello, V.; Peterson, B.W.; van der Mei, H.C.; Busscher, H.J. Physico-chemistry from initial bacterial adhesion to surface-programmed biofilm growth. *Adv. Colloid Interface Sci.* **2018**, *261*, 1–14. [[CrossRef](#)] [[PubMed](#)]

Disclaimer/Publisher’s Note: The statements, opinions and data contained in all publications are solely those of the individual author(s) and contributor(s) and not of MDPI and/or the editor(s). MDPI and/or the editor(s) disclaim responsibility for any injury to people or property resulting from any ideas, methods, instructions or products referred to in the content.